

AD-A137 947

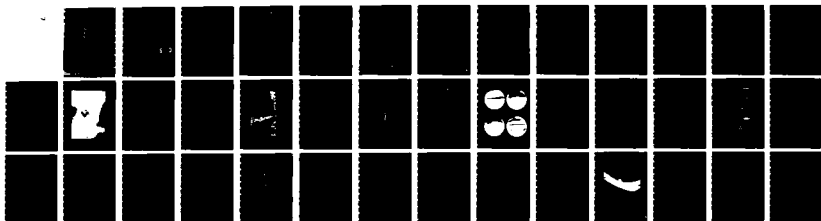
CHATHIKA RADAR AND S3-2 MEASUREMENTS OF AURORAL-ZONE
ELECTRODYNAMICS IN T. (U) SRI INTERNATIONAL MENLO PARK
CA R M ROBINSON NOV 83 SCIENTIFIC-1 AFGL-TR-83-0221
F19628-82-K-0045

1/1

UNCLASSIFIED

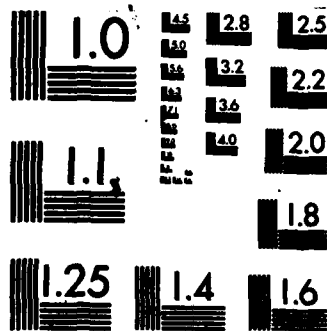
F/G 20/14

NL



END

FILED
3-
DTIC



MICROCOPY RESOLUTION TEST CHART
NATIONAL BUREAU OF STANDARDS-1963-A

AD A137947

AFGL-TR-83-0221

12

**CHATANIKA RADAR AND S3-2 MEASUREMENTS
OF AURORAL-ZONE ELECTRODYNAMICS
IN THE MIDNIGHT SECTOR**

By: ROBERT M. ROBINSON

SRI INTERNATIONAL
333 Ravenswood Avenue
Menlo Park, California 94025

November 1983

*Scientific Report No. 1
For Period 6 July 1982 - 31 October 1983*

DISTRIBUTION STATEMENT A

**Approved for public release
Distribution Unlimited**

**DTIC
ELECTE
FEB 15 1984
S B**

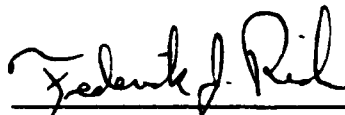
Prepared for: AIR FORCE GEOPHYSICS LABORATORY
AIR FORCE SYSTEMS COMMAND
UNITED STATES AIR FORCE
HANSCOM AFB, MASSACHUSETTS 01731

DTIC FILE COPY

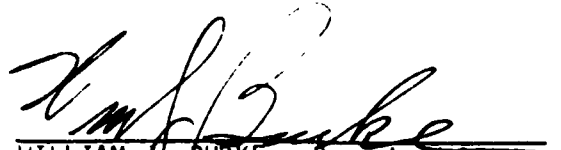
84 02 15 037

This report has been reviewed by the ESD Public Affairs Office (PA) and is releasable to the National Technical Information Services (NTIS).

"This technical report has been reviewed and is approved for publication"

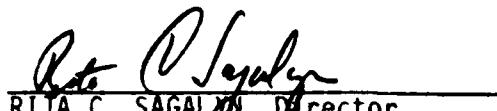


FREDERICK J. RICH
Contract Manager



WILLIAM J. BURKE, Branch Chief
Plasmas, Particles & Fields Branch
Space Physics Division

FOR THE COMMANDER


RITA C. SAGALIN, Director
Space Physics Division

Qualified requestors may obtain additional copies from the Defense Technical Information Center. All others should apply to the National Technical Information Service.

If your address has changed, or if you wish to be removed from the mailing list, or if the addressee is no longer employed by your organization, please notify AFGL/DAA, Hanscom AFB, MA 01731. This will assist us in maintaining a current mailing list.

Do not return copies of this report unless contractual obligations or notices on a specific document requires that it be returned.

UNCLASSIFIED

SECURITY CLASSIFICATION OF THIS PAGE (When Data Entered)

REPORT DOCUMENTATION PAGE		READ INSTRUCTIONS BEFORE COMPLETING FORM
1. REPORT NUMBER AFGL-TR-83-0221	2. GOVT ACCESSION NO. AD-A137947	3. RECIPIENT'S CATALOG NUMBER
4. TITLE (and Subtitle) CHATANIKA RADAR AND S3-2 MEASUREMENTS OF AURORAL-ZONE ELECTRODYNAMICS IN THE MIDNIGHT SECTOR	5. TYPE OF REPORT & PERIOD COVERED Scientific Report No. 1 covering period 6 July 1982 to 31 October 1983	
7. AUTHOR(s) Robert M. Robinson	6. PERFORMING ORG. REPORT NUMBER SRI Project 4592	
9. PERFORMING ORGANIZATION NAME AND ADDRESS SRI International 333 Ravenswood Avenue Menlo Park, California 94025	8. CONTRACT OR GRANT NUMBER(s) F19628-82-K-0045	
11. CONTROLLING OFFICE NAME AND ADDRESS Air Force Geophysics Laboratory Hanscom AFB, Massachusetts 01731 Monitor/Frederick J. Rich/PHG	10. PROGRAM ELEMENT, PROJECT, TASK AREA & WORK UNIT NUMBERS 61102F 2311G2EE	
14. MONITORING AGENCY NAME & ADDRESS (if different from Controlling Office)	12. REPORT DATE November 1983	
	13. NUMBER OF PAGES 40	
	15. SECURITY CLASS (of this report) UNCLASSIFIED	
	15a. DECLASSIFICATION/DOWNGRADING SCHEDULE	
16. DISTRIBUTION STATEMENT (of this Report) Approved for public release; distribution unlimited		
17. DISTRIBUTION STATEMENT (of the abstract entered in Block 20, if different from Report)		
18. SUPPLEMENTARY NOTES		
19. KEY WORDS (Continue on reverse side if necessary and identify by block number) Harang discontinuity, field-aligned currents, S3-2 satellite, Chatanika radar, electric field		
20. ABSTRACT (Continue on reverse side if necessary and identify by block number) Chatanika radar measurements were combined with S3-2 satellite data obtained during passes over the midnight sector auroral zone to study the relationships between conductivities, electric fields, and currents in the Harang discontinuity. Three passes were chosen based on the quality of the radar and satellite data and the availability of supplementary ground-based or satellite measurements. The radar measured electric fields and conductivities as a function of latitude and local time. The satellite measured the -		

DD FORM 1 JAN 73 1473

EDITION OF 1 NOV 65 IS OBSOLETE


UNCLASSIFIED

SECURITY CLASSIFICATION OF THIS PAGE (When Data Entered)

X
UNCLASSIFIED

SECURITY CLASSIFICATION OF THIS PAGE(When Data Entered)

latitudinal distribution of electric field and field-aligned current during the three polar passes. The most intense electric fields were observed in the poleward and equatorward portions of the auroral oval as defined by the region of enhanced ionospheric conductivity. These high electric fields were located at the boundaries between oppositely directed field-aligned-current sheets. The dominant field-aligned-current region in the Harang discontinuity was a broad upward current sheet within which bright auroral arcs were observed. In the three cases examined, there was a net upward current in the discontinuity.



UNCLASSIFIED

SECURITY CLASSIFICATION OF THIS PAGE(When Data Entered)

CONTENTS

LIST OF ILLUSTRATIONS	v
1. INTRODUCTION	1
2. RESULTS OF OBSERVATIONS	5
2.1 Observations on 31 January 1978	5
2.2 Observations on 3 February 1978	11
2.3 Observations on 9 February 1978	19
3. DISCUSSION	25
4. SUMMARY	31
REFERENCES	33

Accession For	
NTIS GRA&I	<input checked="" type="checkbox"/>
DTIC TAB	<input type="checkbox"/>
Unannounced	<input type="checkbox"/>
Justification	
By	
Distribution/	
Availability Codes	
Dist	Avail and/or Special
A-1	

ILLUSTRATIONS

- 1 Perturbations in the H Component of the Magnetic Field Measured by the College Magnetometer on 31 January 1978
- 2 Location of the S3-2 Pass at 1000 UT on 31 January 1978
- 3 DMSP Photograph of the Aurora over Alaska at 1000 UT on 31 January 1978
- 4 S3-2 Data for the Pass on 31 January 1978
- 5 Approximate Location of the Infinite East-West Current Filaments Used in Calculating Ground Magnetic Perturbations from the Radar Electric Field and Conductivity Measurements
- 6 Contour Plot of Electron Density in the Magnetic Meridian Plane Constructed from Radar Data Obtained on 31 January 1978 During an Elevation Scan that was Simultaneous with the S3-2 Pass
- 7 Same as Figure 1 for 3 February 1978
- 8 Sequence of Four All-Sky Camera Images Photographed from Chatanika on 3 February 1978
- 9 Location of the S3-2 Pass over Alaska on 3 February 1978
- 10 Same as Figure 4 for 3 February 1978
- 11 Sequence of Electron Density Contour Plots Obtained from Radar Elevation Scans on 3 February 1978
- 12 Same as Figure 1 for 9 February 1978
- 13 Location of the S3-2 Pass over Alaska on 9 February 1978
- 14 Same as Figure 4 for 9 February 1978
- 15 Vector Plots Showing the Location of the Reversal in Ionospheric Current as Measured by the Radar at Various Times During the Evening of 9 February 1978

- 16 Vector Plots Showing the Location of the Reversal in Ion Drift as Measured by the Radar at Various Times During the Evening of 9 February 1978
- 17 Schematic Diagram of Field-Aligned Currents, Electric Fields, and Aurora in the Midnight Sector

1. INTRODUCTION

The two-cell convection pattern proposed by Axford and Hines [1961] that describes the general movement of plasma in the high-latitude ionosphere has been confirmed by numerous electric-field measurements made by ground and space-borne instruments. The two-cell pattern involves antisunward flow of plasma over the polar cap and sunward flow within the auroral zone. The plasma that convects across the polar cap divides, part of it flowing westward through the evening-sector auroral oval, part flowing eastward through the morning-sector auroral oval. When this flow is projected into the equatorial plane of the magnetosphere, it corresponds to the flow of sunward-moving plasma in the plasma sheet. Because auroral substorms typically begin in this region, the flow can be quite complex and dynamic.

Early studies of ground magnetic perturbations [Harang, 1946] revealed that a discontinuity exists in the ionospheric current flow in the midnight-sector auroral zone. Poleward of the discontinuity the current is westward while equatorward of the discontinuity the current is eastward. The discontinuity is slanted in local time and appears earlier at higher latitudes.

Heppner [1954] established that the transition in the appearance of auroral forms from discrete arcs in the evening hours to diffuse patches in the morning hours occurs near the discontinuity in the current. Davis [1962] showed that the discontinuity also marked the separation between westward drifting auroral forms in the evening sector and eastward drifting auroral forms in the morning sector. Heppner [1972] examined this discontinuity in more detail and named it the Harang discontinuity.

Maynard [1974] systematically studied electric-field measurements in the vicinity of the Harang discontinuity. Using OGO 6 data, he was able to show that the discontinuity is present even during quiet times.

As the magnetic activity increases, the line along which the discontinuity occurs moves equatorward with some shift in the angle of the slant. Maynard [1974] attempted to interpret these changes in terms of plasma flow in the magnetotail.

Electric-field measurements near the Harang discontinuity were also made by Wedde et al. [1977] using the Chatanika incoherent-scatter radar in Alaska. The radar data clearly show that the electric field changes from northward in the evening sector to southward in the morning sector across the discontinuity. The change is seldom abrupt, and more often occurs over several hours of local time. Furthermore, rather than changing discontinuously, the variation often occurs as a counterclockwise rotation of the electric-field vector. Wedde et al. [1977] also found that the electron precipitation increased within the region of the discontinuity.

Iijima and Potemra [1976] described measurements of field-aligned currents in the midnight sector oval. Using data from the Triad satellite, they found that field-aligned currents in the midnight sector were complex with little consistency from pass to pass. The distinction between Region 1 and Region 2 that Iijima and Potemra [1976] made for other local times is not obvious in the midnight sector. Even if the electric-field reversal in the Harang discontinuity is well defined, the field-aligned currents may be much more structured owing to spatial and temporal variations in ionospheric conductivity. To explain the observations, simultaneous measurements of electric field, conductivity, and field-aligned currents must be used. Even such data from polar orbiting satellites may not be sufficient to study these relationships because these measurements are made as a function of latitude only. The nature of the Harang discontinuity may be such that variations in electrodynamic parameters in the east-west direction are significant.

In this report, we use simultaneous measurements made by the S3-2 satellite and the Chatanika radar to study the electrodynamics of the auroral zone in the vicinity of the Harang discontinuity. We have chosen three S3-2 passes over Chatanika from a much larger set of such

passes. The three passes were selected on the basis of the quality of the radar and satellite data and the availability of supplementary ground-based or satellite measurements.

The S3-2 measurements used in this study were obtained by a tri-axial fluxgate magnetometer and a 27.4-m dipole antenna oriented in the spacecraft's spin plane [Burke et al., 1980]. The magnetometer measures perturbations in the geomagnetic field that can be used to infer the magnitude and direction of field-aligned currents. Five-second averages of data from the dipole yield the components of electric field in the trajectory plane. Because the satellite crosses Alaska very nearly along the magnetic meridian, the forward electric field (E forward) reflects the magnitude of the north-south component of the electric field.

For several hours including the time of the S3-2 overpass, the Chatanika radar scanned in elevation in the magnetic meridian. This operating mode allows measuring electron density and ion-drift velocity as a function of both altitude and latitude. From these quantities, we can compute the horizontal electric field, the height-integrated ionospheric conductivity, and the perpendicular current intensity.

There are many advantages of combining satellite measurements with simultaneous measurements made from ground-based instruments. In the present case, we identify three objectives of the combined analysis. First, the satellite measurements are made during one pass approximately along the magnetic meridian. The radar monitors electrodynamic parameters over a long time before, during, and after the time of the pass. Thus, the satellite measurements can be put in the proper perspective based on information the radar provides about the prevailing ionospheric conditions. Second, the satellite provides accurate measurements of electric field and field-aligned current, while the radar measures quantities that are important for studying the closure of these currents. Last, because the satellite pass did not always coincide with the Chatanika meridian, the two measurements of electric field can be used to study the variation in the electric field perpendicular to the meridian plane.

In the following section, we discuss the available data for each of the three S3-2 passes over Chatanika. For each pass, we begin by discussing auroral and geomagnetic conditions. We then present the radar and satellite data and discuss to what extent they can be combined to yield a consistent picture of auroral currents. We present our general conclusions, based on the results of all three passes, in the final section.

2. RESULTS OF OBSERVATIONS

2.1 Observations on 31 January 1978

Figure 1 shows the variations in the H component of the geomagnetic field recorded by the College, Alaska, magnetometer on 31 January 1978.

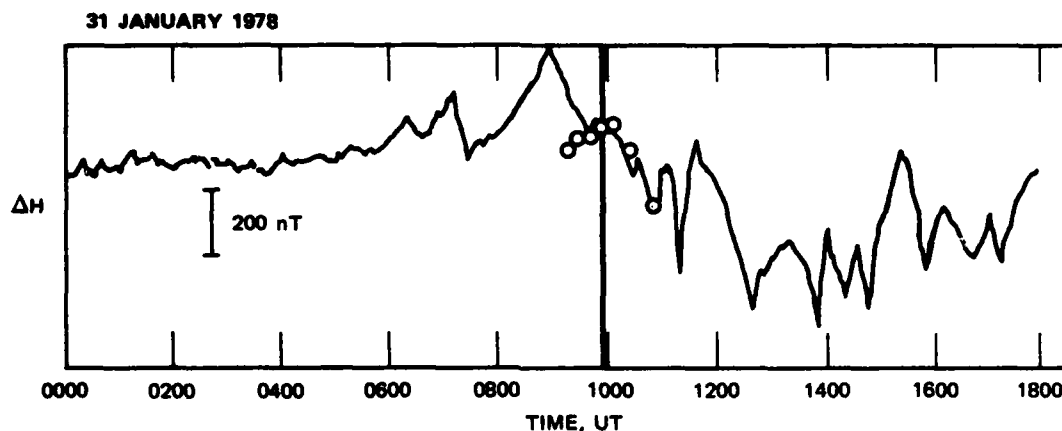


FIGURE 1 PERTURBATIONS IN THE H COMPONENT OF THE MAGNETIC FIELD MEASURED BY THE COLLEGE MAGNETOMETER ON 31 JANUARY 1978

There are two distinct positive bays apparent in the data. The first occurred at about 0700 UT (magnetic local time \sim UT - 11.5 hrs) while the second occurred at 0900 UT. These two events represent intensifications of eastward electrojet activity over College. Examination of magnetometer data from stations north of College revealed that a westward electrojet was situated poleward of the eastward current region. Thus, the Harang discontinuity was north of College during this interval. At 1000 UT, the H component at College becomes negative, which indicates that the discontinuity was over the station. The S3-2 pass over Alaska occurred at about 0957 UT. Figure 2 shows the ground track of the satellite during this pass.

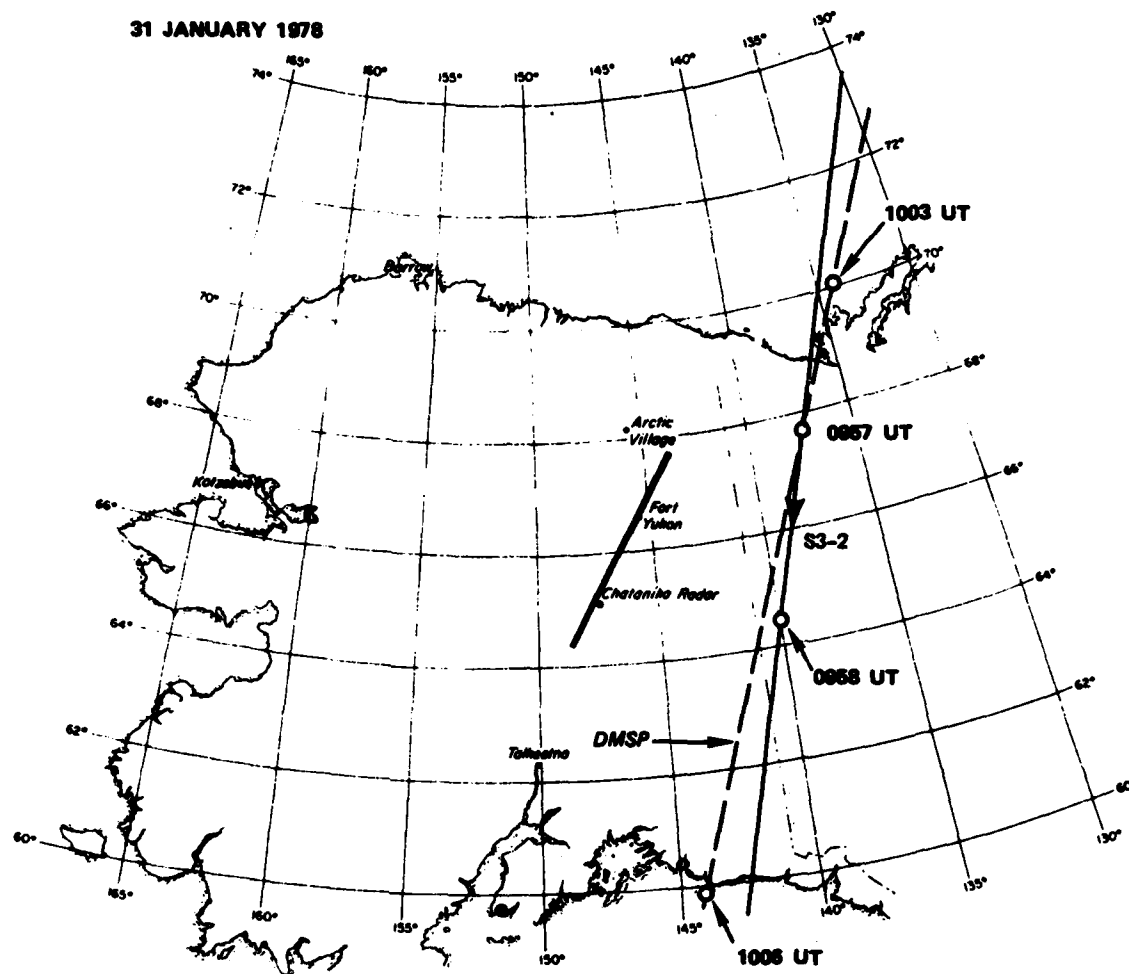


FIGURE 2 LOCATION OF THE S3-2 PASS AT 1000 UT ON 31 JANUARY 1978

Figure 3 is an image obtained by the DMSP F3 satellite during the simultaneous S3-2 pass. The ground track of the S3-2 satellite and the geographic coordinates have also been superimposed on this figure. The location of Chatanika, Alaska, is indicated. It is apparent from the photograph that a broad diffuse aurora was present between 63° and 70° invariant latitude. To the north of the diffuse aurora is an auroral arc containing a large loop or fold. The loop is similar in appearance to a westward traveling surge. Such surges often accompany the substorm expansion phase.

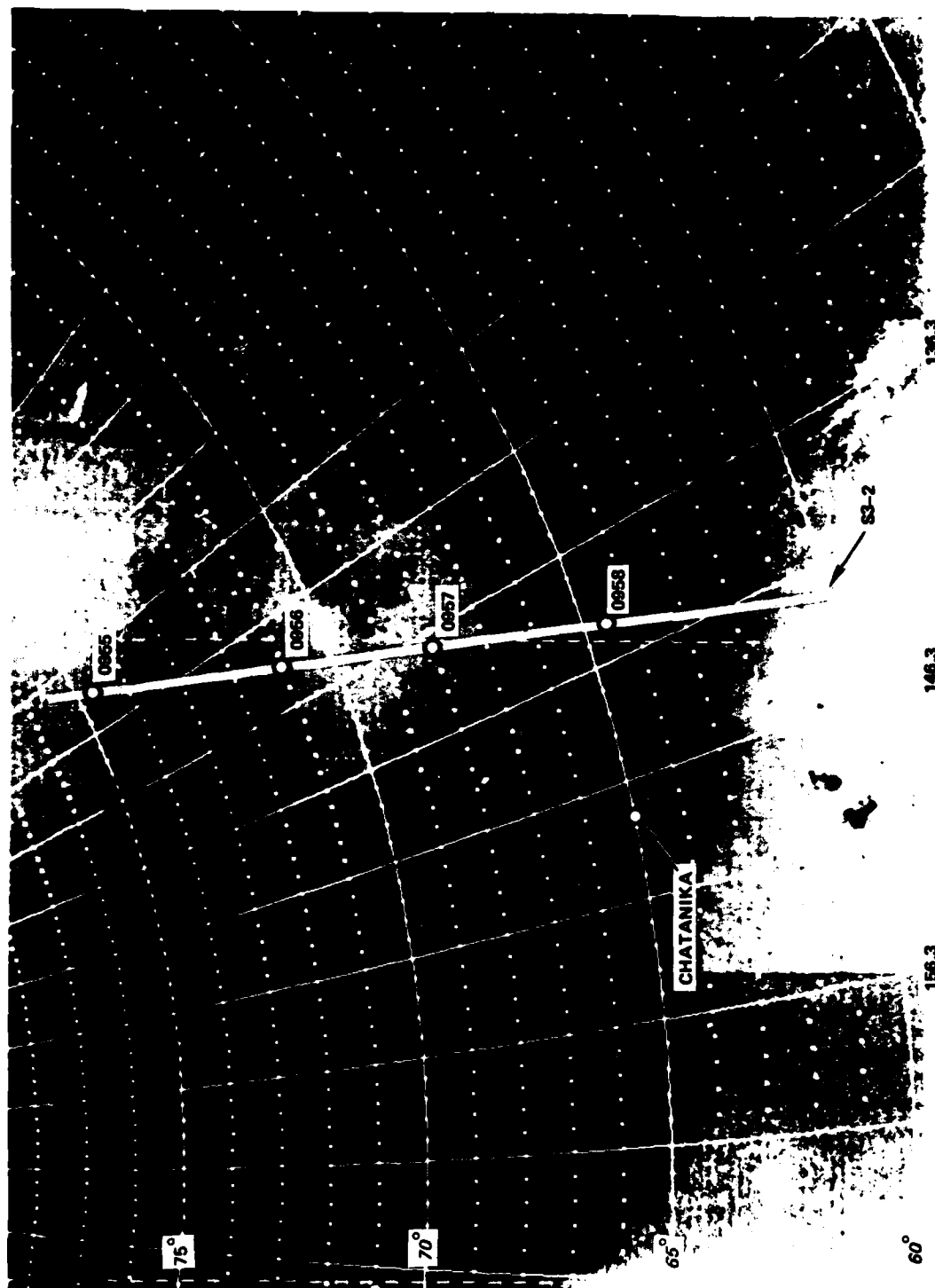


FIGURE 3 DMSP PHOTOGRAPH OF THE AURORA OVER ALASKA AT 1000 UT ON 31 JANUARY 1978

The top panel of Figure 4 shows the S3-2 magnetometer data measured during the satellite pass. The vertical scale gives the east-west magnetic perturbation. As the satellite passes through a field-aligned current sheet, the east-west magnetic perturbation changes depending on the direction and magnitude of the current in the sheets. In Figure 4 (and similar figures to follow), positive slope corresponds to upward field-aligned current, and negative slope corresponds to downward field-aligned current. The magnitude of the slope reflects the intensity of the current sheet. Between 62° and 64° invariant latitude, there is a downward current of about $1 \mu\text{A}/\text{m}^2$. From 64° to 72° , the current is upward at about $0.4 \mu\text{A}/\text{m}^2$. Between 72° and 74° , there is a series of four current sheets, two upward and two downward. The current in each of these sheets exceeds $3 \mu\text{A}/\text{m}^2$. This structured current configuration appears to be associated with the auroral loop shown in Figure 3. Note also that there is a net negative deviation in the magnetometer data indicating that the total upward current integrated across the auroral zone exceeds the total downward current.

The solid trace in the bottom panel of Figure 4 is the forward electric field. Negative electric field in this figure is approximately magnetic northward. The satellite data indicate a region of fairly intense northward electric field at about 60° latitude, well equatorward of the region of significant parallel current. There is also a region of intense southward electric field far to the north.

Radar elevation scans were made starting at 0907 UT and ending at 1048 UT. The electric field and height-integrated conductivity measurements from each of these scans were used to compute the expected perturbation in the H component of the magnetometer at College. Figure 5 shows the geometry of these calculations. The electrojet is assumed to be composed of about 40 east-west current filaments spaced at intervals of 5 to 20 km. The altitude of these filaments is chosen to be 115 km. The ground perturbation in H is computed by summing the contribution from each of these current filaments. Each scan yields one value of the ground H perturbation. The results obtained for 31 January 1978 are superimposed on the magnetometer data in Figure 1. The decrease in H

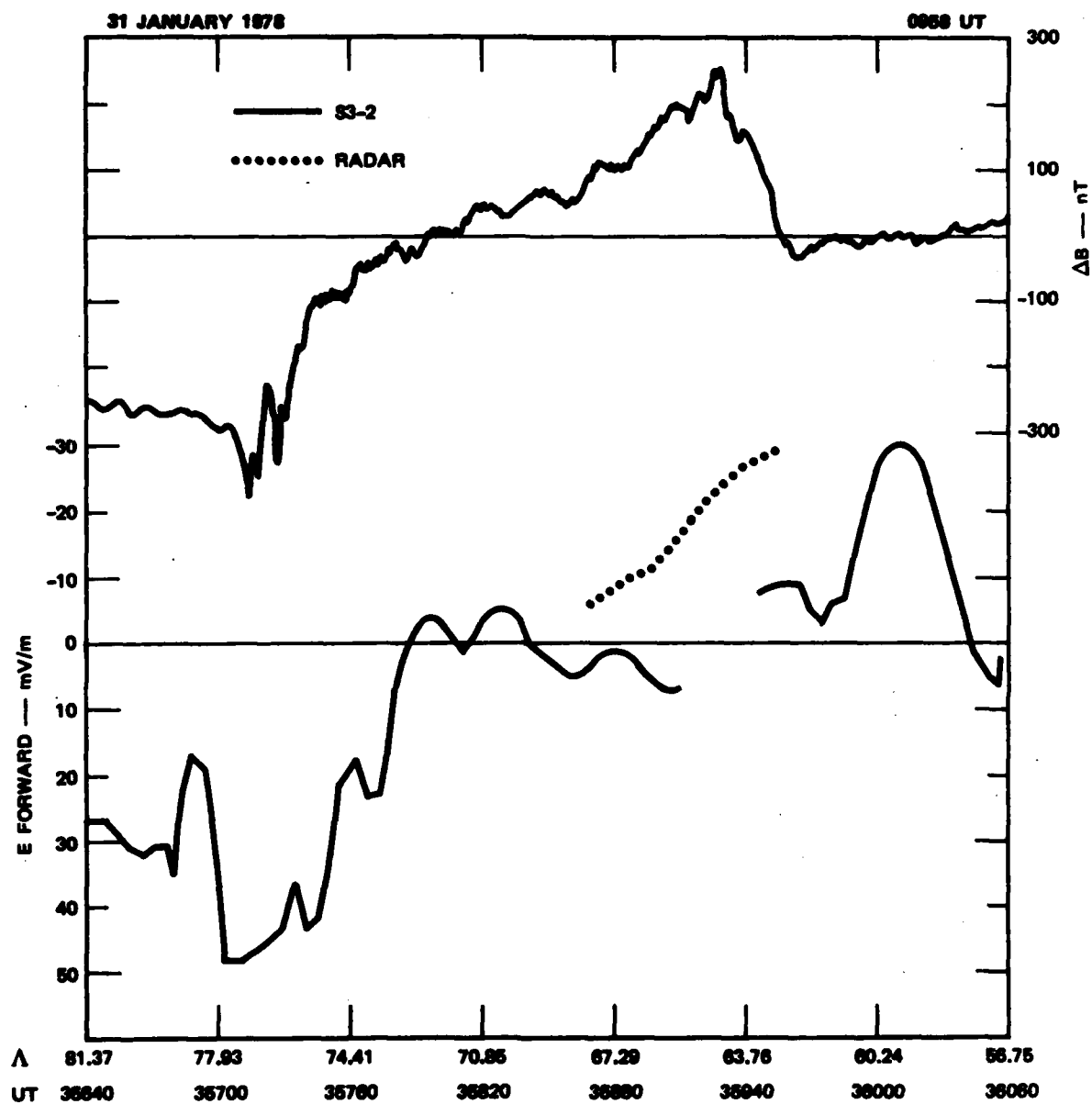


FIGURE 4 S3-2 DATA FOR THE PASS ON 31 JANUARY 1978

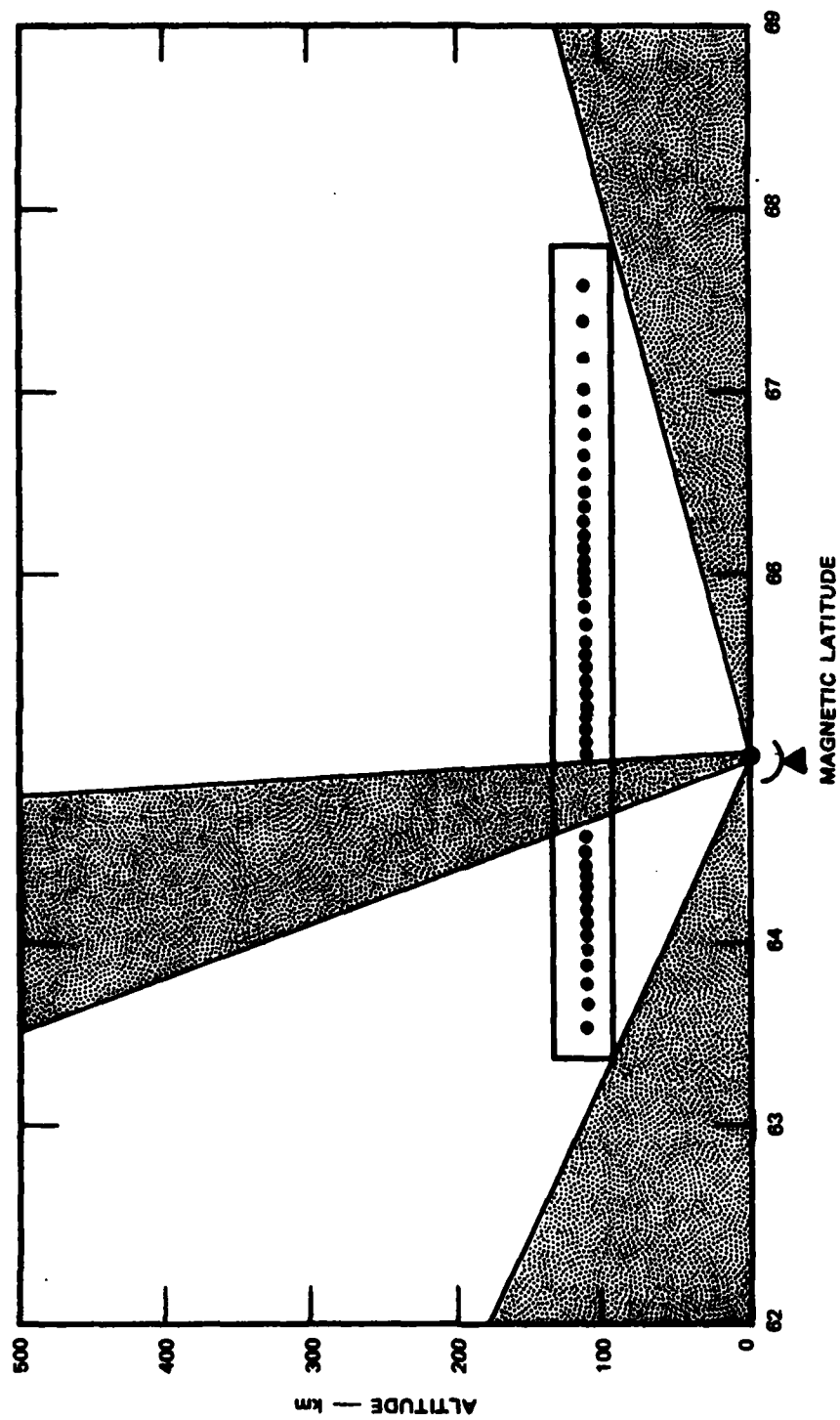


FIGURE 5 APPROXIMATE LOCATION OF THE INFINITE EAST-WEST CURRENT FILAMENTS USED IN CALCULATING GROUND MAGNETIC PERTURBATIONS FROM THE RADAR ELECTRIC-FIELD AND CONDUCTIVITY MEASUREMENTS

with time follows very closely the actual decrease recorded by the College magnetometer. Examination of the radar data shows that the decrease in H shown in Figure 1 is caused primarily by a decrease in the northward electric field over the entire region that the radar sampled. The conductivity on the other hand, remains fairly constant.

Figure 6 is an electron-density contour plot constructed from radar data obtained during the scan that was simultaneous with the satellite pass. The ionization is fairly uniform with one density maximum at a latitude of 65° . The electric-field measurements made by the radar during this scan are shown as a dotted trace in the bottom panel of Figure 4. The radar electric fields are larger than those measured simultaneously by the satellite. A possible explanation is that the difference represents a spatial variation in the electric field between the radar meridian and the S3-2 satellite path.

2.2 Observations on 3 February 1978

Figure 7 shows the H component recorded by the College magnetometer on 3 February 1973. Two isolated negative bays are apparent. The first has an abrupt onset at about 1130 UT. However, enhanced magnetic activity is apparent as early as 0600 UT. The second bay occurred at about 1500 UT. The S3-2 satellite pass on this evening occurred between 1021 and 1024 UT, or just before the onset of the first large negative bay at College.

Figure 8 shows all-sky camera photographs taken from Chatanika during this satellite pass. Before the pass, an isolated arc was nearly at the radar's zenith, with additional arcs far to the north. As the satellite passed over, this arc drifted northward and seemed to coalesce with the other arcs to the north creating a wide band of luminosity that stretched from just north of the zenith to the northern horizon. The region just overhead was less luminous than the arc region to the north and the diffuse aurora to the south. The auroral activity shown in this sequence is fairly typical of the activity throughout much of the evening before 1500 UT when the second bay occurred. That is, for most of

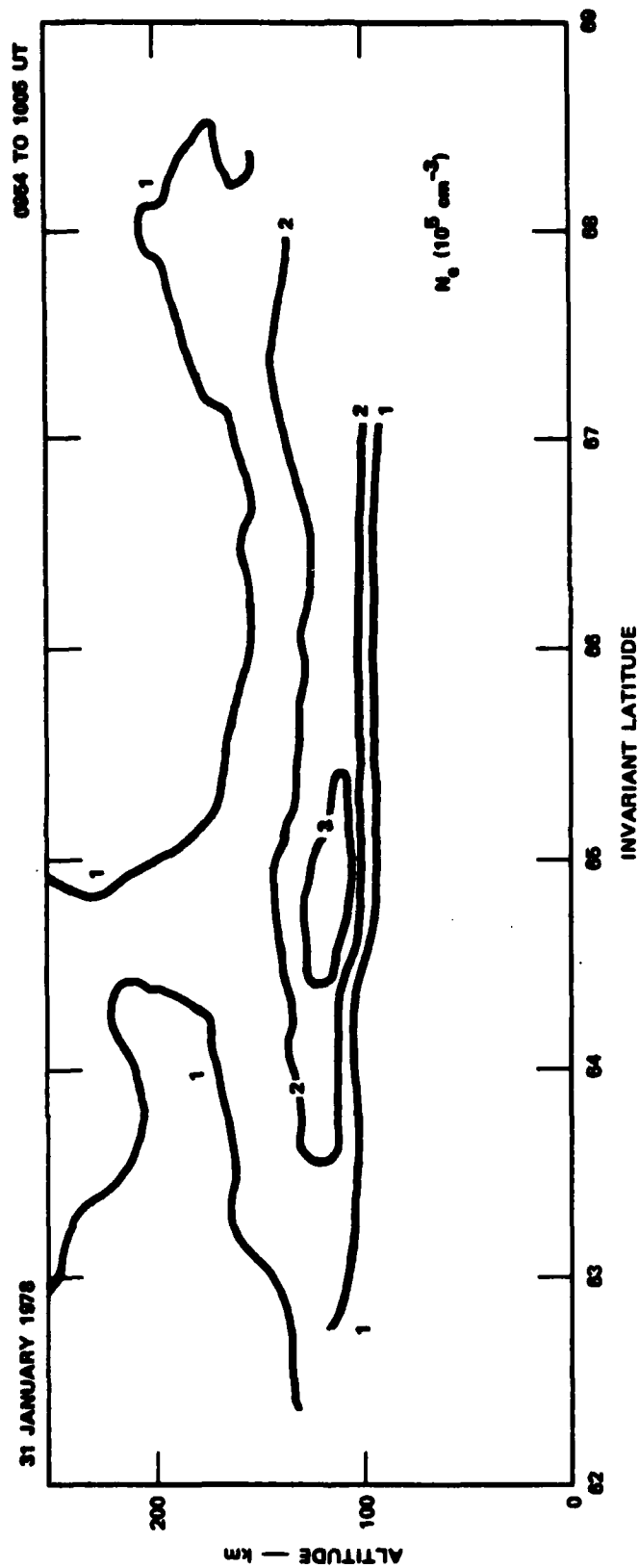


FIGURE 6 CONTOUR PLOT OF ELECTRON DENSITY IN THE MAGNETIC MERIDIAN PLANE CONSTRUCTED FROM RADAR DATA OBTAINED ON 31 JANUARY 1978 DURING AN ELEVATION SCAN THAT WAS SIMULTANEOUS WITH THE S3-2 PASS

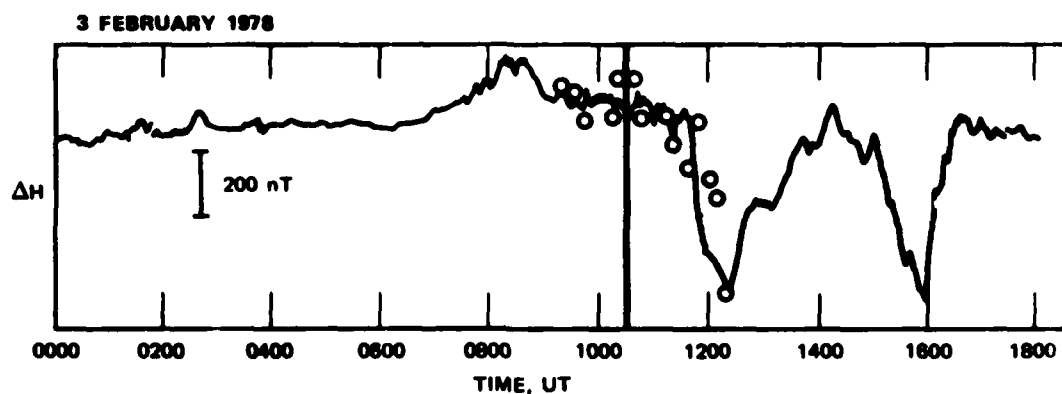


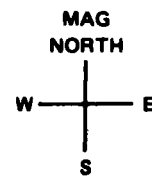
FIGURE 7 PERTURBATIONS IN THE H COMPONENT OF THE MAGNETIC FIELD MEASURED BY THE COLLEGE MAGNETOMETER ON 3 FEBRUARY 1978

the evening, auroral luminosity was confined to drifting auroral bands oriented approximately in the magnetic east-west direction.

Figure 9 shows the ground track of the S3-2 satellite over Chatanika. The satellite passed directly over Fort Yukon and was within 50 km of the radar at closest approach. The upper trace in Figure 10 shows east-west magnetic perturbations measured by the satellite magnetometer. There is a downward current of about $3 \mu\text{A}/\text{m}^2$ between 64.4° and 65.4° latitude. Poleward of this current sheet is a less intense upward current with an average current density of $0.8 \mu\text{A}/\text{m}^2$. This current sheet extends to about 71° latitude and, thus, coincides with the broad region of auroral luminosity apparent in the all-sky camera photographs. There is evidence in the magnetometer data that a third current sheet exists poleward of the upward current. As in the data for 31 January 1978, there is a shift in the level of the baseline that suggests a net upward field-aligned current.

The satellite electric-field data are shown as a solid trace in the bottom panel of Figure 10. These data show a region of southward electric field to the north and northward electric field to the south. The region in between coincides roughly with the region of enhanced luminosity. The extent of the enhanced precipitation during this pass can be

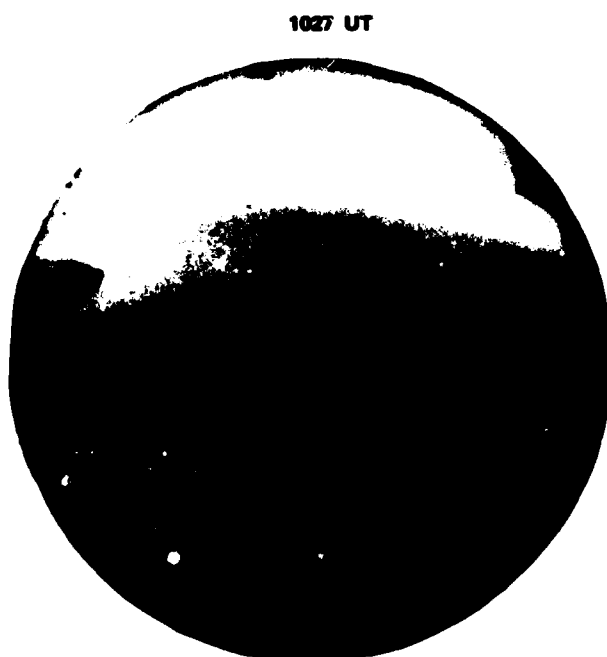
3 FEBRUARY 1978



1017 UT



1022 UT



1027 UT



1032 UT

FIGURE 8 SEQUENCE OF FOUR ALL-SKY CAMERA IMAGES PHOTOGRAPHED FROM CHATANIKA ON 3 FEBRUARY 1978

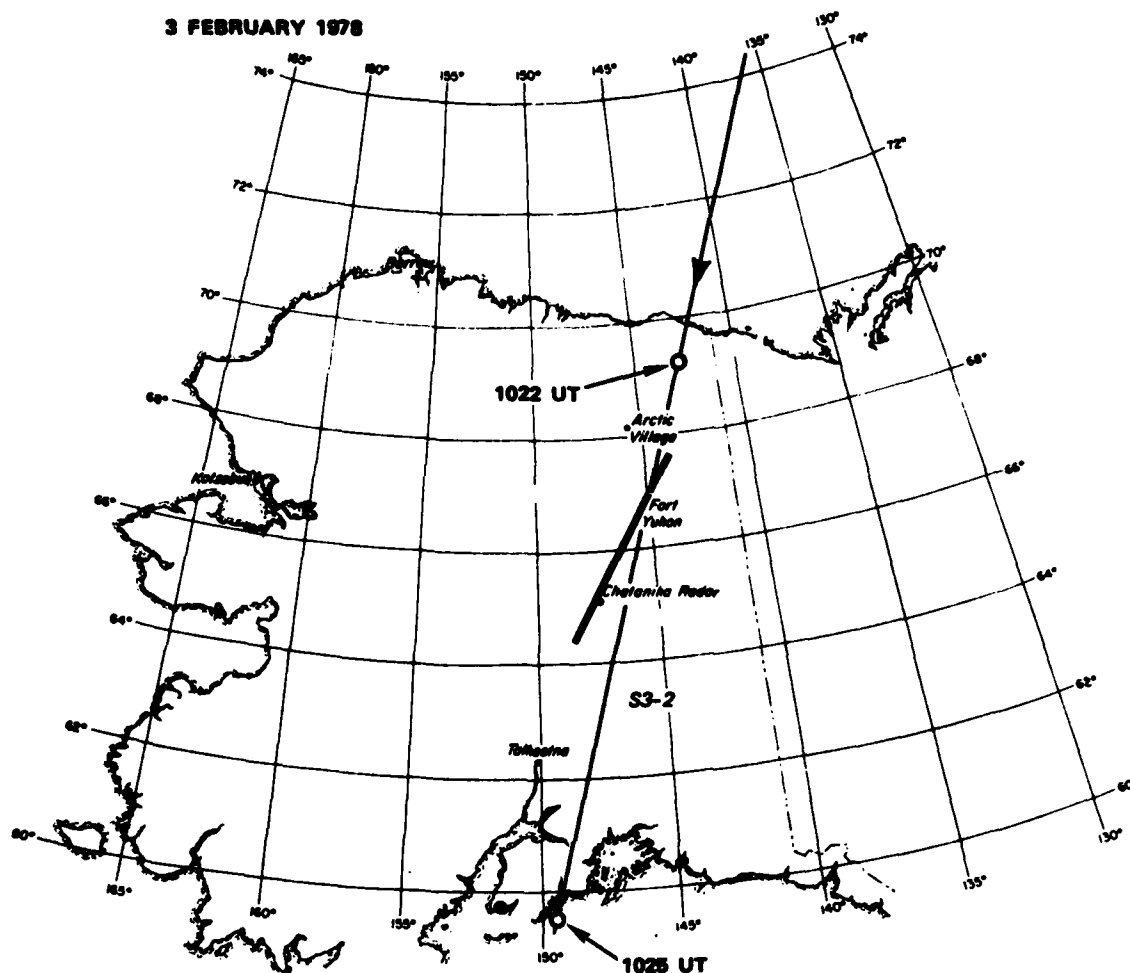


FIGURE 9 LOCATION OF THE S3-2 PASS OVER ALASKA ON 3 FEBRUARY 1978

determined by examination of the S3-2 electron spectrometer data. These data show that the energy flux carried by precipitating electrons exceeded $0.5 \text{ ergs/cm}^2\text{-sec}$ between 65.3° and 70.7° invariant latitude.

Radar elevation scans were made between 0913 and 1222 UT on the evening of 3 February 1978. The H component of the College magnetogram was computed by the method discussed above, and the results shown as open circles in Figure 7. Before 1100 UT, the magnetic deflection was positive indicating the presence of a weak eastward electrojet over

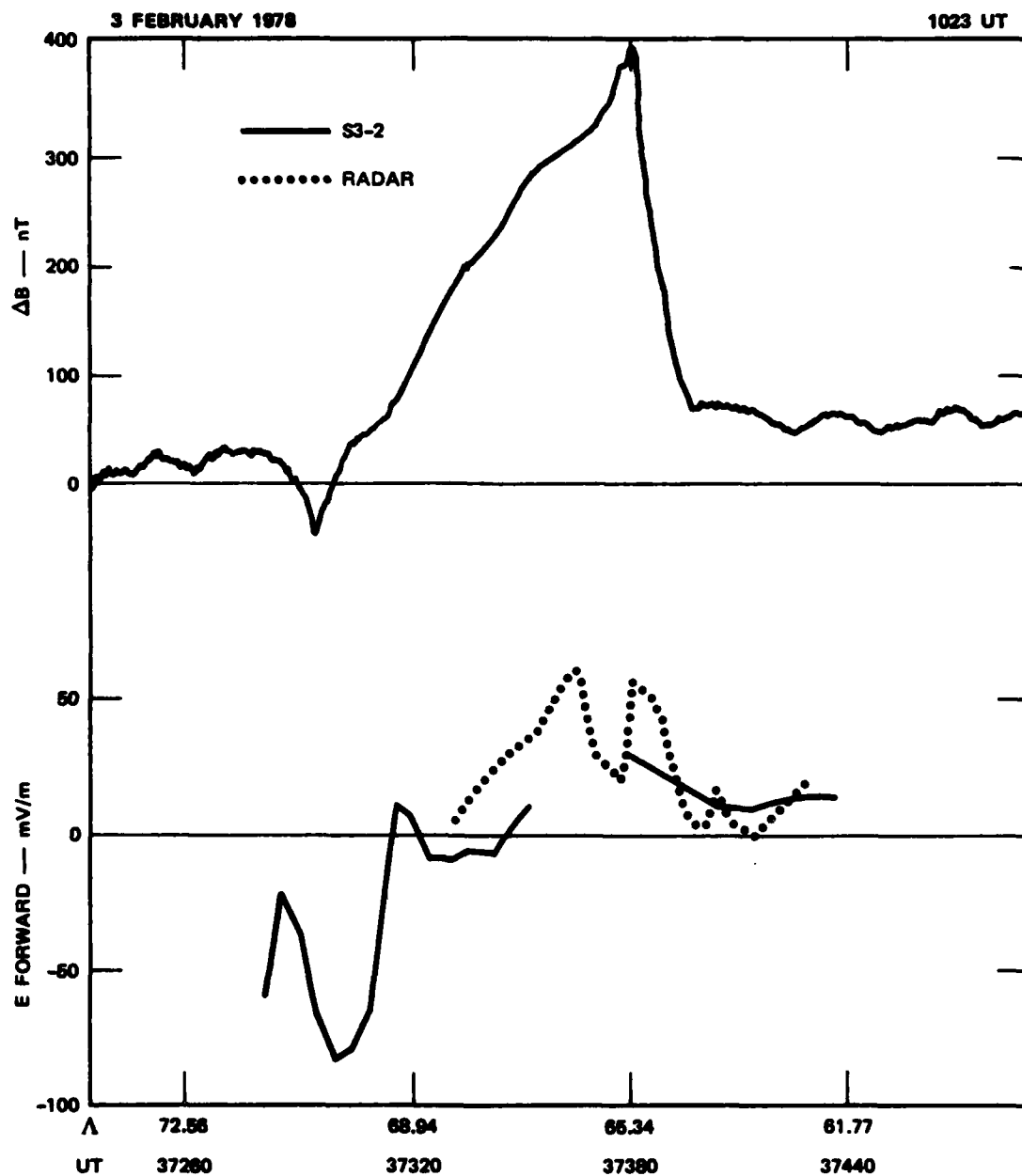


FIGURE 10 S3-2 DATA FOR THE PASS ON 3 FEBRUARY 1978

College, which agrees with the ground magnetometer data. At 1100 UT, the current reversed and a negative H perturbation was produced.

Figure 11 shows electron density contour plots constructed from radar data obtained during selected scans between 0913 and 1105 UT. The scan made between 1017 and 1029 UT was simultaneous with the satellite pass. However, some caution should be used in comparing the radar data for this scan with the satellite data. The radar was pointing northward at the start of the scan. The all-sky camera photographs show that at this time the region north of the radar contained no auroral arcs. By 1021 UT, however, this region is filled in by the auroral arc that has drifted northward from the zenith. Because the satellite pass occurred after 1021 UT, the satellite detected auroral precipitation throughout the region north of the radar. A better comparison between the radar and satellite can probably be made using data from the following scan. As shown in Figure 11, by the time this later scan was made, the auroral luminosity had spread considerably.

Examination of the electron density contour plots from scans between 0913 and 1100 UT revealed the consistent presence of three ionospheric features. These features are apparent in the contour plots from selected scans shown in Figure 11. To the south was a region of enhanced ionization approximately 1° wide. The maximum density in this enhancement varied between 1 and 2×10^5 el/cm^3 . The enhancement appears to be fairly uniform in the east-west direction because the ionization, width and location changes only very little from one scan to the next. We associate this enhancement with the diffuse aurora that is apparent in the all-sky camera photographs. A second feature that is apparent in all the scans is the auroral arc. Although the maximum density, width, and location of the arc varies considerably, its location relative to the diffuse aurora is fairly constant. In fact, the all-sky camera photographs show that on that evening auroral arcs typically formed just poleward of the diffuse aurora, then drifted slowly northward. At least two of these drifting arcs could be seen by examining the photographs. The third feature, we identify in the elevation scan data is the dark band that typically separates the diffuse aurora and the auroral arc. This band warrants identification for two reasons:

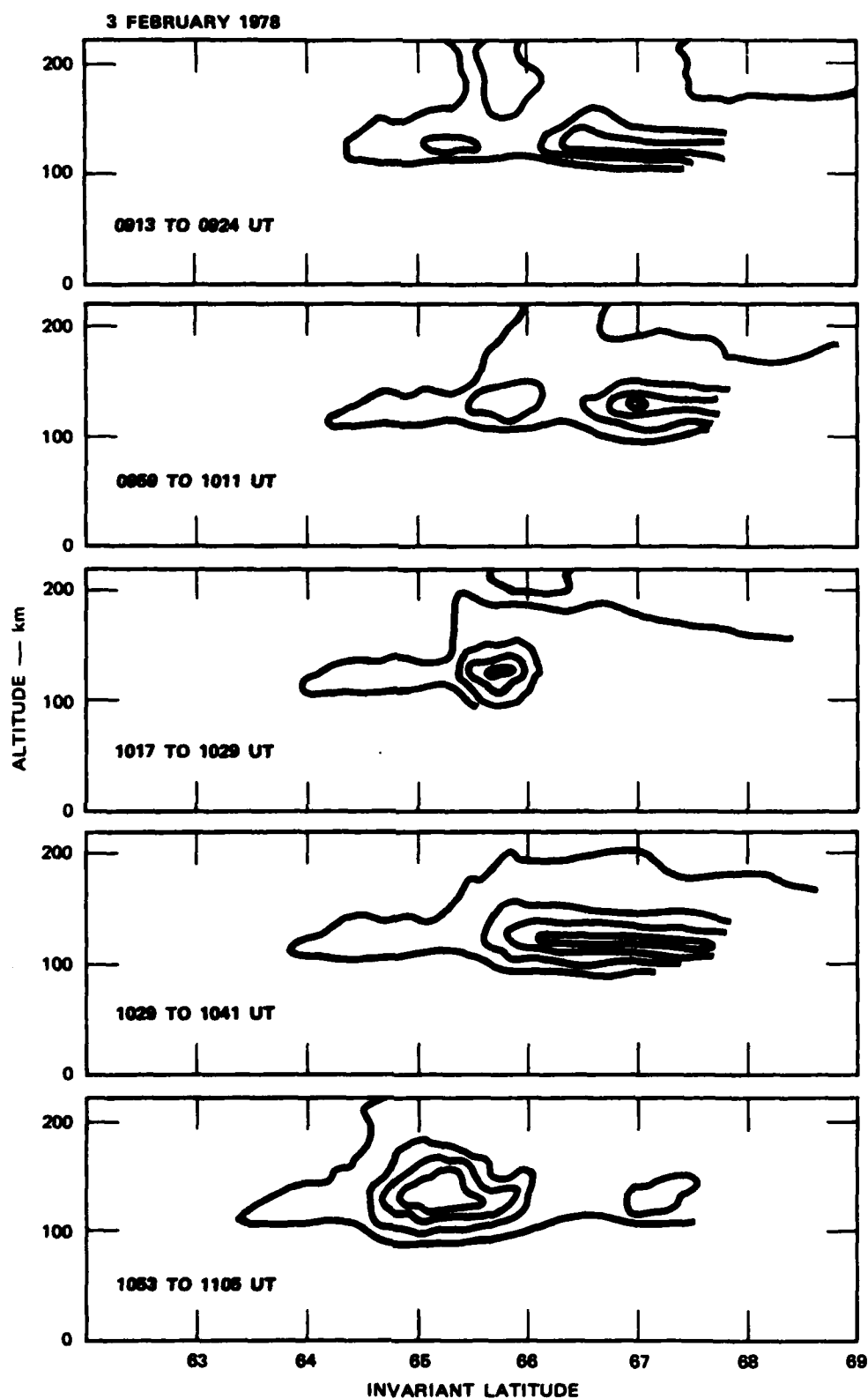


FIGURE 11 SEQUENCE OF ELECTRON DENSITY CONTOUR PLOTS OBTAINED FROM RADAR ELEVATION SCANS ON 3 FEBRUARY 1978

- (1) It is virtually always present. That is, in none of the scans did the auroral arc occur far enough south to obscure the density maximum associated with the diffuse aurora: the two maxima were always separate, with the dark band lying in between.
- (2) The northward electric field maximizes within the dark band. Thus, the dark band may carry significant horizontal current, despite the low conductivities. In addition, because of the high electric fields, the ionospheric Joule heating maximizes in the dark band.

The electric field measured by the radar is shown as a dotted trace in the bottom panel of Figure 10 for comparison with the satellite measurements. These measurements agree reasonably well with those made by the satellite.

2.3 Observations on 9 February 1978

Figure 12 shows the perturbations in the H component of the magnetic field recorded by the College magnetometer on 9 February 1978.

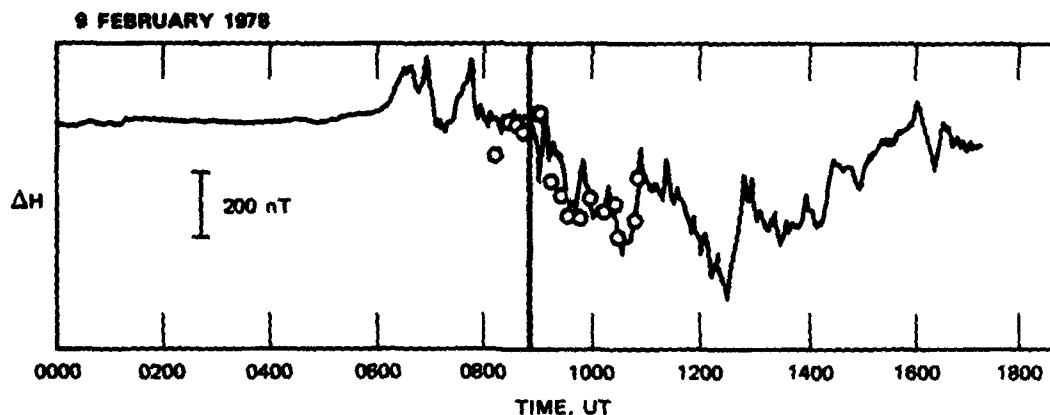


FIGURE 12 PERTURBATIONS IN THE H COMPONENT OF THE MAGNETIC FIELD MEASURED BY THE COLLEGE MAGNETOMETER ON 9 FEBRUARY 1978

Before 0830 UT, the perturbations indicated a positive bay at College. Magnetic stations to the north recorded negative perturbations. Examination of magnetic records from other stations in the Alaska chain revealed that the separation between the eastward electrojet to the south

and the westward electrojet to the north was situated approximately between Inuvik and Arctic Village, or, equivalently, between 71° and 73° invariant latitude. After 0830 UT, the westward electrojet moved to lower latitudes. The reversal in electrojet direction is obvious in the College magnetometer trace.

Figure 13 shows the location of the S3-2 ground track during a pass near Chatanika at about 0930 UT on 9 February. Note the large separa-

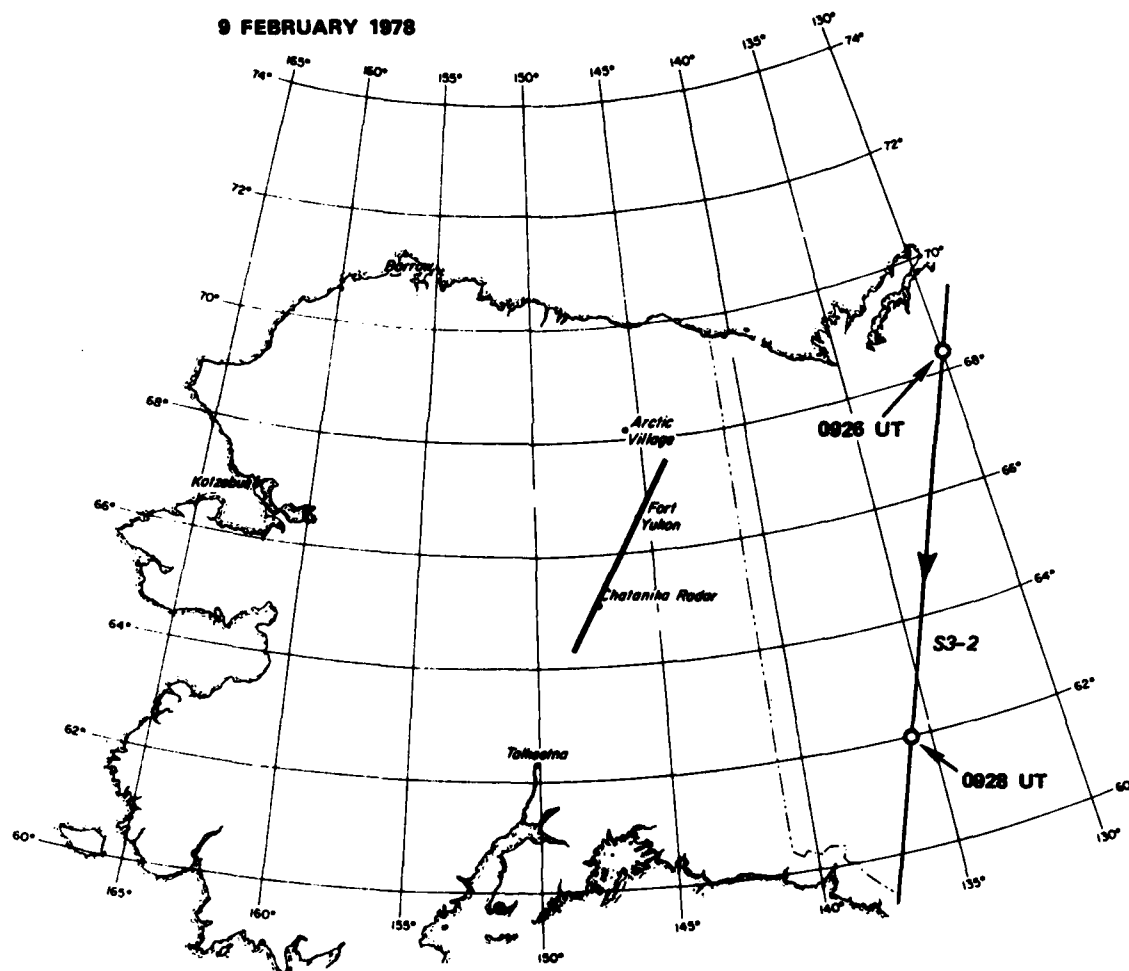


FIGURE 13 LOCATION OF THE S3-2 PASS OVER ALASKA ON 9 FEBRUARY 1978

tion between the satellite and the Chatanika meridian. Figure 14 shows data from the satellite for this pass. The east-west magnetic

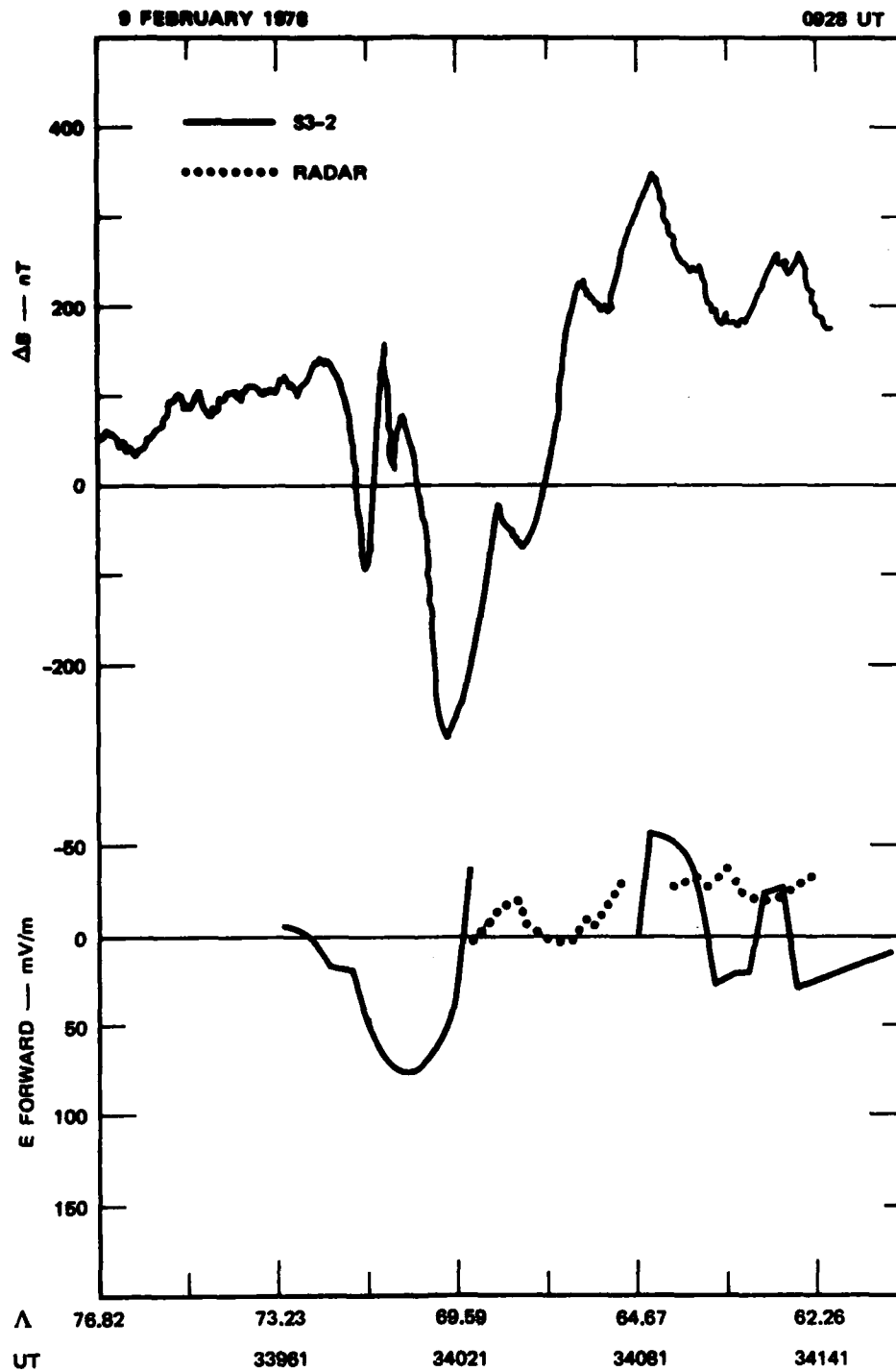


FIGURE 14 S3-2 DATA FOR THE PASS ON 9 FEBRUARY 1978

perturbations measured by the magnetometer are shown in the upper trace. The field-aligned currents implied by these variations are quite complex. Ignoring the small-scale variations, we can discern three major current sheets. Most prominent is the region of upward current that extends between 65.7° and 69.6° latitude. On either side of this wide current sheet there are downward current sheets. In addition there is another up-down current pair centered at about 71° latitude. Note once again that the baseline shift in the magnetometer trace indicates a net upward current from the ionosphere.

The satellite electric-field measurements are shown as a solid trace in the lower panel of Figure 14. The most prominent feature is the intense southward electric field located just poleward of the upward current sheet.

Radar measurements of electric field and conductivity on the evening of 9 February were used to calculate the expected perturbations in the College magnetometer. The results are shown in Figure 12. Note that the radar data reproduce the transition from positive bay to negative bay that occurs at about 0930 UT, the time of the S3-2 pass. Figure 15 shows vectorially the direction and magnitude of the ionospheric current measured during five consecutive elevation scans. In the first scan, a weak westward electrojet is situated between 67° and 68° poleward of the eastward electrojet, which is wider and more intense. In the succeeding scans, the westward electrojet broadens to the south and intensifies until, by 1020 UT, no eastward current remains in the radar field of view. Figure 16 shows the plasma velocity vectors for these five scans. The convection reversal is quite distinct in these data. Figure 14 shows the radar electric-field measurements for the scan that was simultaneous with the S3-2 satellite pass. There is no evidence for a southward electric field in these data; however, this is not surprising because the southward electric-field region apparent in the satellite data was probably far to the east.

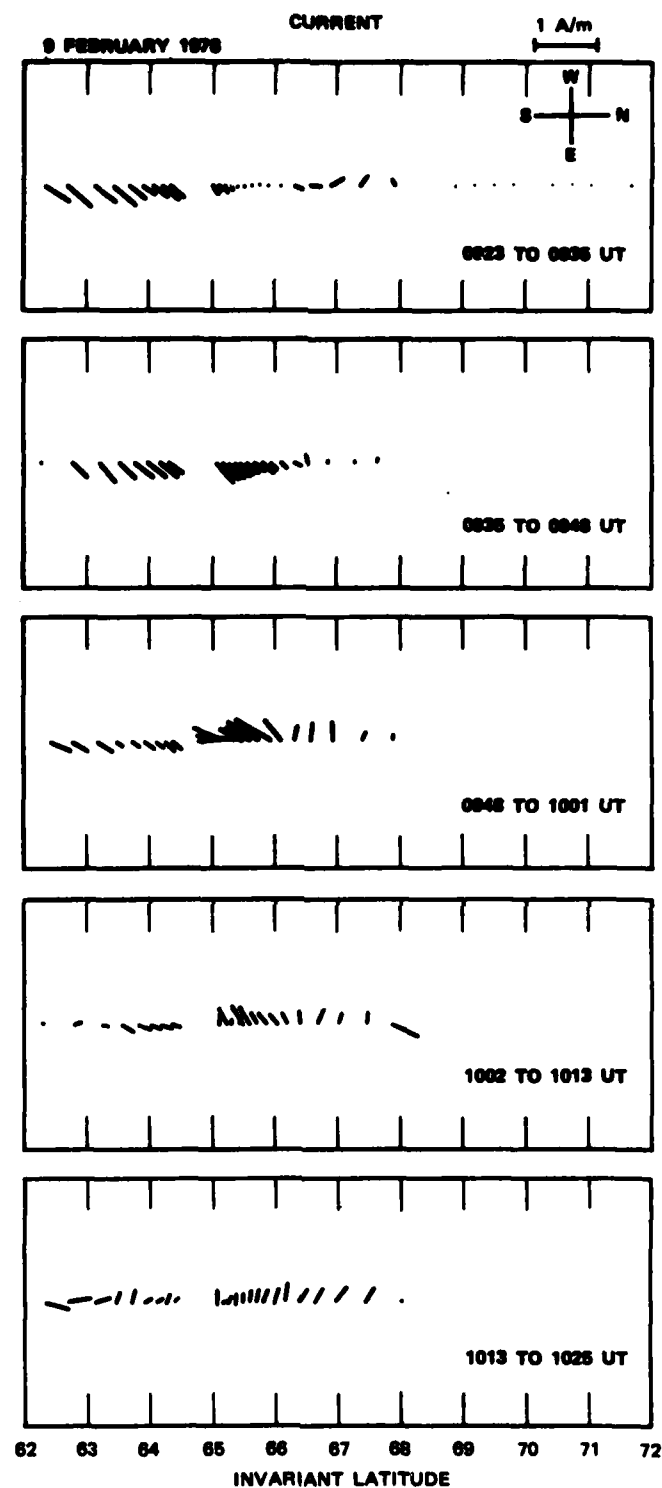


FIGURE 15 VECTOR PLOTS SHOWING THE LOCATION OF THE REVERSAL IN IONOSPHERIC CURRENT AS MEASURED BY THE RADAR AT VARIOUS TIMES DURING THE EVENING OF 9 FEBRUARY 1978

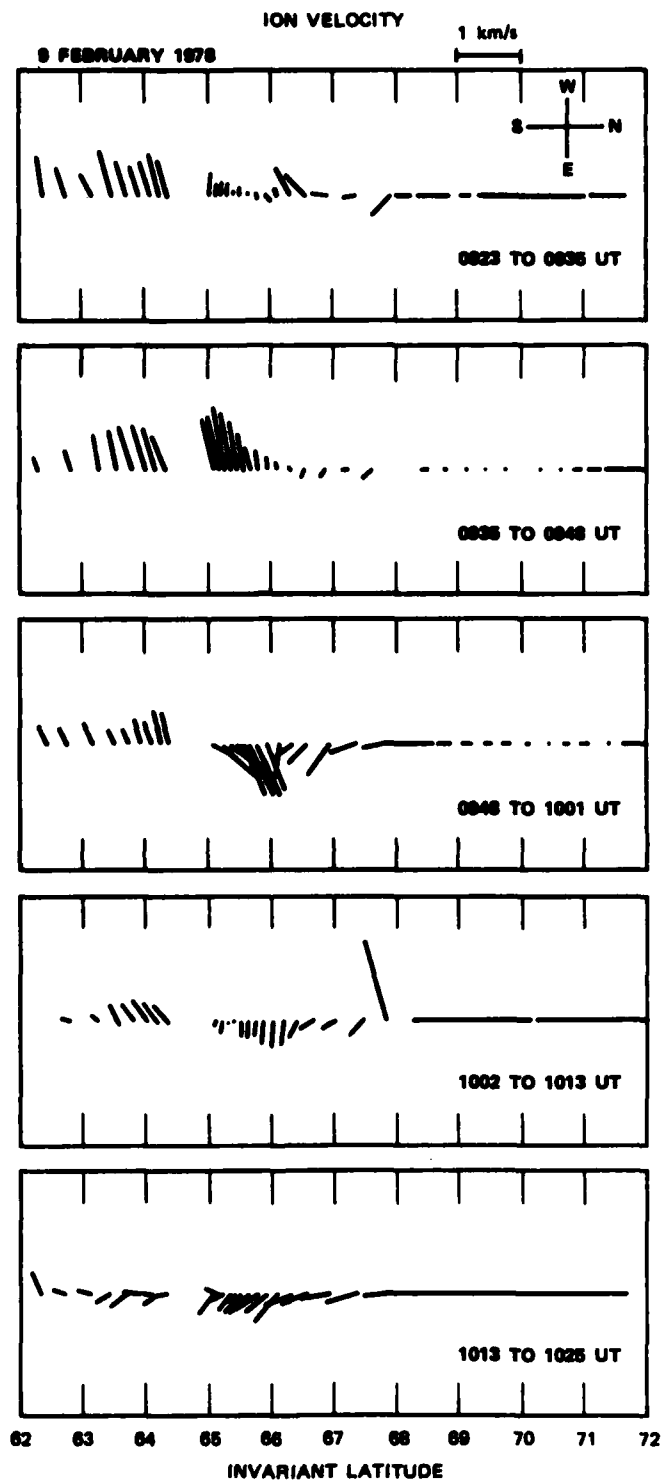


FIGURE 16 VECTOR PLOTS SHOWING THE LOCATION OF THE REVERSAL IN ION DRIFT AS MEASURED BY THE RADAR AT VARIOUS TIMES DURING THE EVENING OF 9 FEBRUARY 1978

3. DISCUSSION

Before discussing the results obtained here, it is important to consider the possible effects of temporal variations in the data. Maynard [1974] showed that the Harang discontinuity exists during all levels of magnetic activity, the only obvious change being its equatorward displacement during more active times. This is somewhat surprising when we consider the tremendously dynamic aurora that occur in association with substorms. In addition, Wiens and Rostoker [1975] found that the westward electrojet extends poleward and westward in steps during the substorm expansion phase. These steplike changes occur in connection with the appearance of a westward traveling surge.

In spite of the dramatic changes, it is possible that the Harang discontinuity can remain unperturbed with only a shift in location because the westward electrojet and westward traveling surge are usually confined to the poleward portion of the expanded auroral oval. These features may be quite dynamic without necessarily changing the structure of field-aligned currents and electric fields in the equatorward portions. The data from 31 January 1978 discussed below exemplify this situation. We will proceed with the discussion assuming that the Harang discontinuity is always present and well defined. We add to this the assumption that the discontinuity changes in location and slant on time scales that are long compared with the duration of a satellite pass. The radar measurements require more careful interpretation because the discontinuity may change often during the time it takes the earth to rotate under it.

There are a few obvious similarities in the S3-2 electric-field and field-aligned-current data for the three passes presented above. In all three cases, a three-sheet field-aligned-current pattern is discernible. The equatorward sheet is narrow and downward, the middle sheet is broad and upward, and the poleward sheet is narrow and downward. The poleward

current sheet is most difficult to identify because of the presence of narrower, multiply-reversing current sheets embedded within. For 31 January 1978, we were able to use a simultaneous DMSP photograph to show that the multiply-reversing current sheets were probably a result of the intense electron precipitation producing the auroral loop to the north. Evidence for a similar structure is present in the data for 9 February 1978. On 3 February 1978, no such narrow current sheets are apparent, and the three-sheet pattern is obvious. We conclude from these considerations that the normal field-aligned-current pattern in the Harang discontinuity consists of a broad upward sheet flanked by two downward sheets. This pattern may be considerably perturbed by the presence of intense precipitation. This precipitation is usually confined to the poleward portion of the field-aligned-current region. The magnetometer data from the three passes also suggest that more upward current flows in the midnight sector than downward current when integrated across the entire field-aligned current sheet.

The electric-field patterns are somewhat more complex than the field-aligned currents, but there are some features common to all three data sets. Most striking is the poleward region of intense southward electric field. Especially interesting with regard to this southward field is its collocation with the boundary between the broad upward current sheet and the downward sheet to the north. On 31 January 1978 and 3 February 1978, the most intense southward electric field coincided with the minimum perturbation in ΔB . This coincidence is not apparent in the data for 9 February 1978. However, we might argue that the unperturbed field-aligned-current pattern on 9 February 1978 would have had a minimum coincident with the electric-field peak, but, because of intense electron precipitation, this pattern was substantially altered.

A second feature in the electric-field data is the northward electric field to the south. This is most apparent in the data for 31 January 1978. The location of the northward electric field in all three cases is near the equatorward boundary of the upward current sheet. In addition, the northward electric field is separated from the region of southward electric field by three to ten degrees of latitude within which the electric field is small.

Because only one component of the electric field is measured by the satellite, there is no information about the transverse component. The region of small E forward may correspond to the region where the electric field rotates through the west. Thus, our data clearly show that the discontinuity is spread out in latitude as pointed out by Wedde et al. [1977]. The small electric field is also consistent with the presence of upward field-aligned current. We expect that the electric field will be small in regions of enhanced conductivity. The increased conductivity in this region is apparent in the radar data for all three passes.

Thus far, we have only discussed the latitudinal variations in electric field and field-aligned currents. To examine the local time variation, we use the radar data, being careful not to confuse temporal and spatial effects.

The radar measurements for 31 January 1978 were made between 0907 and 1100 UT. There was no evidence for an electric-field reversal throughout this time. Yet the College magnetometer recorded a change in the direction of the H component of the geomagnetic field. The only way to resolve this discrepancy is to assume that an intense westward electrojet was situated in the north just out of the radar field of view. This westward electrojet may have been driven by the strong southward electric field to the north. Thus, although the radar did not observe the electric field reversal, there is strong evidence for its presence in the far north.

The differences in the electric fields measured simultaneously by the satellite and the radar and shown in Figure 4 suggest that there was a local time variation of the field. As shown in Figure 3, the radar was displaced from the magnetic meridian by about 400 km. From these data, it appears that the region of northward electric field is broader to the west than to the east. If we associate an eastward electrojet with this northward electric field region, we conclude that the eastward electrojet narrows in a wedge-shaped manner in the vicinity of the Harang discontinuity.

Information on the local-time structure of the Harang discontinuity can also be inferred from the data obtained on 9 February 1978. The time of the S3-2 pass corresponds closely to the time of reversal in the H component of the College magnetometer. The reversal in the electric field is apparent in the radar data from the scan made between 0948 and 1002 UT, just after the S3-2 pass. Because the pass was located to the east of the radar, the satellite must have traversed the eastern portion of the Harang discontinuity. Further indication of this is contained in the S3-2 magnetometer data, which differs significantly from the magnetometer data obtained during the passes on 3 February 1978 and 31 January 1978. The field-aligned-current configuration on 9 February 1978 resembles that typically found in the morning-sector auroral oval. That is, the upward current sheet is situated equatorward of the downward current sheet. There is some evidence for the presence of an additional downward current sheet on the equatorward side, but this sheet is certainly not as prominent as it is on the other two days. Thus, the transition from the evening-sector field-aligned-current configuration to the morning-sector configuration takes place across the Harang discontinuity. The change occurs by way of a decrease in intensity of the equatorward current sheet and a corresponding increase in intensity of the poleward sheet. Both poleward and equatorward sheets are downward with a much wider upward current sheet situated between them.

The radar data obtained on 3 February 1978 cannot be used to determine the local time variation of the electric field because the S3-2 pass was almost coincident with the magnetic meridian through Chatanika. However, the electron density contour plots obtained on this day can be used to relate the field-aligned currents and electric fields in the Harang discontinuity to source regions of precipitating electrons in the magnetosphere.

The latitudinally broad maximum in E region ionization at 64° invariant latitude in Figure 11 is similar in appearance to the feature referred to as the interface arc by Robinson et al. [1982]. Robinson et al. [1982] presented evidence suggesting that this ionization feature is produced by precipitating electrons from the central plasma sheet.

Referring to Figure 10, it is clear that this precipitation is situated on field lines that carry downward field-aligned currents. The upward current region within which the bright auroral arcs are seen probably extends to the distant magnetotail. Winningham et al. [1975] have referred to this region as the boundary plasma sheet. The large southward electric field at the poleward edge of the current sheet probably marks the polar cap boundary.

4. SUMMARY

The features of the Harang discontinuity inferred from the data discussed above have been incorporated in Figure 17. The illustration shows, qualitatively, the relationship between aurora, electric fields, and field-aligned currents.

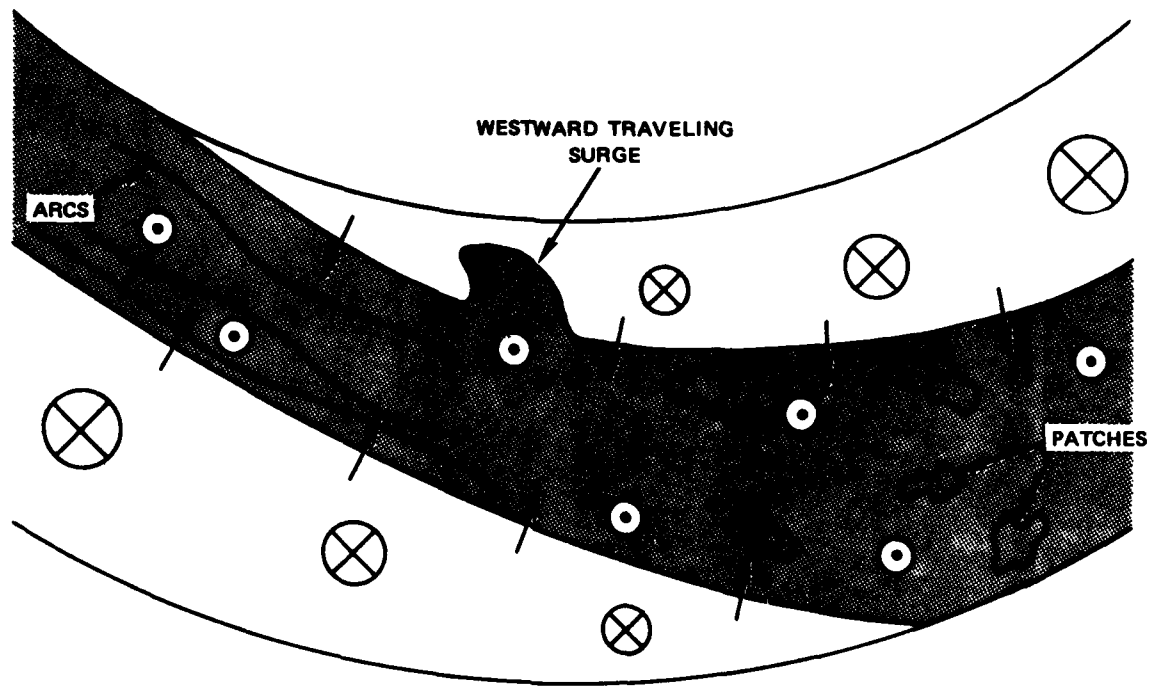


FIGURE 17 SCHEMATIC DIAGRAM OF FIELD-ALIGNED CURRENTS, ELECTRIC FIELDS, AND AURORA IN THE MIDNIGHT SECTOR. The arrows indicate the directions of the most intense electric fields. The shaded region indicates upward field-aligned current.

and field-aligned currents. We find that the most intense electric fields are located in the poleward and equatorward portions of the auroral oval. The peak electric fields occur at the boundaries between current sheets. However, the poleward boundary of the upward current sheet is often perturbed owing to the presence of intense electron precipitation. The downward current sheets that flank the broad upward

current sheet decrease in intensity in the vicinity of the discontinuity. This decrease is represented in Figure 17 by the diameter of the circles that indicate the direction of the current. In the three cases we examined, there was a net upward current out of the discontinuity. The upward current region was the site of drifting auroral arcs in the evening sector. In the morning sector, the aurora is disconnected and patchy. The westward traveling surges occur at the poleward edge of the upward current sheet.

REFERENCES

- Axford, W. I., and C. O. Hines (1961), "A Unifying Theory of High-Latitude Geophysical Phenomena and Geomagnetic Storms," Can. J. Phys., Vol. 39, p. 1433.
- Burke, W. J., D. A. Hardy, F. J. Rich, M. C. Kelley, M. Smiddy, B. Schuman, R. C. Sagalyn, R. P. Vancour, P. J. L. Wildman, and S. T. Lai (1980), "Electrodynamic Structure of the Late Evening Sector of the Auroral Zone," J. Geophys. Res., Vol. 85, p. 1179.
- Davis, T. N. (1962), "The Morphology of the Auroral Displays of 1957-1958, 2. Detail Analysis of Alaska Data and Analysis of High-Latitude Data," J. Geophys. Res., Vol. 67, p. 75.
- Harang, L. (1946) "The Mean Field of Disturbance of Solar Geomagnetic Storms," Terr. Magn. Atmos. Elec., Vol. 51, p. 353.
- Heppner, J. P. (1954) "A Study of Relationships Between the Aurora Borealis and the Geomagnetic Disturbances Caused by Electric Currents in the Ionosphere," Ph.D. Thesis, California Institute of Technology, Pasadena, CA.
- Heppner, J. P. (1972), "The Harang Discontinuity in Auroral Belt Ionospheric Currents," Geophys. Publ., Vol. 29, p. 105. p. 105.
- Iijima, T., and T. A. Potemra (1978), "Large-Scale Characteristics of Field-Aligned Currents Associated with Substorms," J. Geophys. Res., Vol. 83, p. 599.
- Maynard, N. C. (1974), "Electric Field Measurements Across the Harang Discontinuity," J. Geophys. Res., Vol. 79, p. 4620.
- Robinson, R. M., R. R. Vondrak, and T. A. Potemra (1982), "Electrodynamic Properties of the Evening Sector Ionosphere Within the Region 2

Field-Aligned Current Sheet," J. Geophys. Res., Vol. 87,
p. 731.

Wedde, T., J. R. Doupnik, and P. M. Banks (1977), "Chatanika Observations of the Latitudinal Structure of Electric Fields and Particle Precipitation on November 21, 1975," J. Geophys. Res., Vol. 82, p. 2743.

Wiens, R. G., and G. Rostoker (1975), "Characteristics of the Development of the Westward Electrojet During the Expansive Phase of Magnetospheric Substorms," J. Geophys. Res., Vol. 80,
p. 2109.

Winningham, J. D., F. Yasuhara, S.-I. Akasofu, and W. J. Heikkila (1975), "The Latitudinal Morphology of 10 eV to 10 KeV Electron Fluxes During Magnetically Quiet and Disturbed Times in the 2100-0300 MLT Sector," J. Geophys. Res., Vol. 80, p. 3148.

END

FILMED

3-84

DTIC